© 2017. Published by The Company of Biologists Ltd | Journal of Cell Science (2017) 130, 1274-1284 doi:10.1242/jcs.197269

RESEARCH ARTICLE

Mitochondrial depolarization in yeast zygotes inhibits clonal expansion of selfish mtDNA

Iuliia E. Karavaeva[1], Sergey A. Golyshev[2], Ekaterina A. Smirnova[2], Svyatoslav S. Sokolov[2], Fedor F. Severin[2] and Dmitry A. Knorre[2,*]

ABSTRACT

Non-identical copies of mitochondrial DNA (mtDNA) compete with each other within a cell and the ultimate variant of mtDNA present depends on their relative replication rates. Using yeast *Saccharomyces cerevisiae* cells as a model, we studied the effects of mitochondrial inhibitors on the competition between wild-type mtDNA and mutant selfish mtDNA in heteroplasmic zygotes. We found that decreasing mitochondrial transmembrane potential by adding uncouplers or valinomycin changes the competition outcomes in favor of the wild-type mtDNA. This effect was significantly lower in cells with disrupted mitochondria fission or repression of the autophagy-related genes *ATG8*, *ATG32* or *ATG33*, implying that heteroplasmic zygotes activate mitochondrial degradation in response to the depolarization. Moreover, the rate of mitochondrially targeted GFP turnover was higher in zygotes treated with uncoupler than in haploid cells or untreated zygotes. Finally, we showed that vacuoles of zygotes with uncoupler-activated autophagy contained DNA. Taken together, our data demonstrate that mitochondrial depolarization inhibits clonal expansion of selfish mtDNA and this effect depends on mitochondrial fission and autophagy. These observations suggest an activation of mitochondria quality control mechanisms in heteroplasmic yeast zygotes.

KEY WORDS: mtDNA, Uncoupler, Heteroplasmy, Mitophagy, Mitochondrial dynamics, ATG32

INTRODUCTION

Eukaryotic cells usually carry multiple copies of mitochondrial DNA (mtDNA). However, due to replication errors, cells can harbor mtDNAs with slightly or significantly different sequences. Such a condition is usually referred to as heteroplasmy (for reviews, see Kmiec et al., 2006; Stewart and Chinnery, 2015). Different variants of mtDNAs compete with each other and the ratios change over generations (He et al., 2010; Solignac et al., 1983) or with age of individual organisms (Taylor et al., 2014). The displacement of the wild-type mtDNA, which encodes a full set of RNAs and proteins, by mutant mtDNA with deleterious mutations can be detrimental for the cells (Aanen and Maas, 2012; Ye et al., 2014). Such displacement plays an important role in the development of mitochondrial genetic diseases and aging (Greaves et al., 2014; for a review, see also Taylor and Turnbull, 2005). Why does the displacement occur? While the changes of mtDNA ratios can be a result of a random genetic drift (Wonnapinij et al., 2008), large mtDNA deletions can also accelerate replication of the mutated molecules.

Baker's yeast *Saccharomyces cerevisiae* is a suitable model for studying competition between different mtDNA variants. Yeast cells can proliferate without functional mtDNA by relying only on glycolysis. At the same time, yeast zygotes inherit mtDNAs from both gametes (for a review, see Contamine and Picard, 2000). For this reason, mating of haploid cells with different mtDNA produces heteroplasmic diploids, which become homoplasmic after a few rounds of cell division (Ling and Shibata, 2004). Competition advantage of the mutant (*rho*$^{-}$) mtDNA over the wild-type mtDNA (*rho*$^{+}$) is usually measured as the proportion of homoplasmic *rho*$^{-}$ diploid descendants in the total number of diploid progeny. This parameter, called suppressivity, can be in the range of 0–100% (Ephrussi et al., 1955) and represents the relative selfishness of the mtDNA variant. It is suggested that the suppressivity level depends strongly on the density and activity of replication origins (*ori*) in the mutant mtDNA molecule (de Zamaroczy et al., 1981). Indeed, small mtDNA molecules with a high density of *ori* sites replicate faster than full-length mtDNA and eventually displace it (see Lorimer et al., 1995). It was also shown that the copy numbers of hypersuppressive mtDNA are much higher than those of the full-length mtDNA (Fangman et al., 1989).

Is it possible to change the competition outcome between mtDNAs by changing mitochondrial function to select in favor of the wild-type mtDNA? Under normal conditions, mammalian cells repeatedly perform quality control of their mitochondrial networks. They remove mitochondria with low transmembrane potential by means of mitophagy, and this removal is mediated by the PINK/Parkin protein system (Twig et al., 2008). *S. cerevisiae* lack PINK/Parkin machinery; their quality control of mitochondria is instead orchestrated by asymmetric distribution of functional and damaged organelles between the mother and the daughter cells (Higuchi-Sanabria et al., 2016; Pernice et al., 2016). Yeast cells also possess a mechanism for mitophagy, but so far this machinery was reported to be used mainly for non-selective, bulk removal of mitochondria in the stationary phase or under nitrogen starvation (for a review, see Müller et al., 2015) and was not shown to be activated by uncouplers (Mendl et al., 2011). At the same time, it was suggested that mitochondrial inner membrane region can be enriched with the proteins encoded by the mtDNA adjacent to this region (the CoRR hypothesis, see Allen, 2015 for a review). Therefore, coupling of mitochondria quality control and negative selection of mutated mtDNAs is theoretically possible. We suggest that, in yeast cells under normal conditions, mitochondrial transmembrane potential is above a threshold that allows discrimination between 'functional' and mutated mtDNAs with decreased respiratory chain activity.

[1]Faculty of Bioengineering and Bioinformatics, Moscow State University, Leninskiye Gory 1-73, Moscow 119991, Russia. [2]Belozersky Institute of Physico-Chemical Biology, Moscow State University, Leninskiye Gory 1-40, Moscow 119991, Russia.

*Author for correspondence (knorre@belozersky.msu.ru)

S.A.G., 0000-0002-4877-1061; S.S.S., 0000-0002-1395-8862; D.A.K., 0000-0001-7468-6963

Received 9 September 2016; Accepted 9 February 2017

Journal of Cell Science (2017) 130, 1274-1284 doi:10.1242/jcs.197269

Thus, treating eukaryotic cells with protonophores might increase the selectivity in favor of functional mtDNA.

In this work, we show that the uncouplers are able to change the outcome of the competition between the wild-type and highly selfish mtDNA variants. We found that this effect depends on mitochondrial dynamics and on the mitophagy receptor Atg32. Moreover, we found that heteroplasmic yeast zygotes have upregulated levels of mitochondrial degradation by autophagy.

RESULTS

Uncouplers increase percentages of *rho*$^+$ diploid progeny of heteroplasmic zygotes

To generate a model system to study selfish mtDNA propagation, we selected a spontaneous *rho*$^-$ mutant with high suppressivity (*HS rho*$^-$, a high proportion of *petite* colonies among the diploid progeny). To estimate the levels of mtDNA selfishness, we mated the *HS rho*$^-$ strain with a wild-type *rho*$^+$ (*WT rho*$^+$) strain and determined the percentage of progeny that had *rho*$^+$ mtDNA (Fig. 1A). Many generations of *HS rho*$^-$ strain did not affect the reproducibility of the results (Fig. S1). We determined the type of mtDNA inherited by the diploid yeast cells by analyzing the colony phenotype. *S. cerevisiae* cells containing the wild-type mtDNA form large colonies (*grande* phenotype, Fig. 1B), while the cells containing mutant non-functional mtDNA (and thus that are respiratory incompetent) form small colonies (*petite* phenotype) when grown on solid medium containing 2% glycerol and 0.1% glucose as carbon source. Loss of HS mtDNA in the *HS rho*$^-$ strain induced by incubation with ethidium bromide (EtBr, see Material and Methods) resulted in a significant decrease of suppressivity (Fig. 1B). Consistent with this, it has been shown previously that crosses to the *rho*^{0} yeast mutant (i.e. yeast without any mtDNA) do not result in a high level of suppressivity (Michaelis et al., 1971). Thus, the high proportion of *petite* diploid progeny in the *HS rho*$^-$×*WT rho*$^+$ mating was not due to a dominant mutation in the nuclear DNA in the *HS rho*$^-$ strain but due to the high suppressivity of its mtDNA. Finally, we selected a set of oppositely directed primers (Table S1) that produced PCR product with *HS rho*$^-$ DNA matrix but not with wild-type mtDNA. Sequencing of *HS rho*$^-$ DNA using these primers allowed us to map the preserved sequence of the *HS rho*$^-$ DNA on yeast mtDNA (Fig. 1C).

To ask whether the zygotes possess mechanisms opposing propagation of selfish mtDNA, we used a number of different compounds known to affect mitochondrial functioning. We tested the ability of these compounds to increase the percentage of *rho*$^+$ progeny in *HS rho*$^-$×*WT rho*$^+$ crossings. We found that mating of *HS rho*$^-$ with *rho*$^+$ in the presence of the uncoupler carbonyl cyanide-4-(trifluoromethoxy)phenylhydrazone (FCCP; 1 µM) significantly increases the proportion of *grande* diploid colonies (Fig. 1B,D). A similar result was obtained with another uncoupler – pentachlorophenol (PCP) (Fig. 1D). This effect was also found with other spontaneous *rho*$^-$ strains (Fig. 1E).

Importantly, the effect of the uncouplers was not the result of a selection against forming diploid *petite* cells. Although uncoupler FCCP slightly decreased the efficiency of mating (Fig. S2), such a weak effect cannot explain the more than 15-fold increase in the proportion of *grande* diploid colonies. Treating *HS rho*$^-$ cells with FCCP (1 µM) did not induce the loss of mtDNA (less than 0.1% *rho*^{0} cells were detected in *HS rho*$^-$×*rho*$^+$ suspensions both in the presence or the absence of FCCP treatment) and therefore the effect of the uncouplers was not because of *rho*^{0} mutation of *rho*$^-$ strains. Moreover, the effect of FCCP on the percentage of *grande* colonies was mostly due to an increase in the numbers of *grande* colonies (Fig. S2). This latter point is important because the *petite* cells would be expected to be more sensitive to uncouplers than *grande* ones. Thus, a possible inhibitory effect on *petite* cells cannot explain our observations.

Anionic uncouplers, such as FCCP, dissipate both components of mitochondrial transmembrane potential – ΔpH and ΔΨ. To find the component responsible for the effect of the uncouplers on mtDNA inheritance, we performed *HS rho*$^-$×*rho*$^+$ mating in the presence of the K^+ uniporter valinomycin to dissipate ΔΨ but not ΔpH. We also assessed the effect of the H^+/K^+ antiporter nigericin to lower the transmembrane ΔpH. In these experiments, nigericin did not affect the percentage of *rho*$^+$ progeny, but the addition of valinomycin resulted in a significant increase in *rho*$^+$ diploid progeny (Fig. 1D). Notably, we found that positively charged dodecyltriphenylphosphonium (C12TPP) did not prevent the expansion of HS mtDNA in the diploids. It was suggested that such compounds induce mitochondrial depolarization but preserve the level of transmembrane potential above the minimum level required for ATP synthesis (see discussion in Severin et al., 2010). One may argue that the observed effect is due to an unspecific decrease in the ATP-to-ADP ratio in the produced zygotes. However, treating the cells with the ATP-synthase inhibitor oligomycin A did not increase the percentage of *rho*$^+$ diploids. Another possible explanation of the effect is that dysfunctional mitochondria induce oxidative stress causing damage of *rho*$^+$ mitochondrial DNA in heteroplasmic zygotes. If this is the case, antioxidants would be expected to increase the percentage of *grande* colonies in our experimental system. However, neither lipophilic antioxidant α-tocopherol nor soluble antioxidant N-acetylcysteine (NAC) caused any significant decrease of suppressivity (Fig. 1D). Thus, our data show that mitochondrial depolarization in heteroplasmic cells acts to decelerate clonal expansion of the mutated HS variant of mtDNA.

Mitochondrial dynamics is required for the effect of the uncouplers on the suppressivity

Why does FCCP prevent the formation of diploid *petite* colonies? One possibility is that the uncouplers prevent fusion of mitochondria from *HS rho*$^-$ and *rho*$^+$ gametes in the zygotes. This could preserve separated mitochondria without HS mtDNA and in this way increase the probability that cells lacking HS mtDNA form following the division of the zygotes. Previously, it was shown *in vitro* that uncouplers prevent fusion of inner mitochondrial membranes (Meeusen et al., 2004). We found that, in the zygotes, FCCP (1 µM) slightly affected mitochondrial fusion (Fig. 2A,B); however the effect (~2-fold increase in the percentages of zygotes with impaired mitochondrial fusion) is obviously too weak to explain the strong (more than 10-fold) increase in the numbers of *grande* colonies in *HS rho*$^-$×*rho*$^+$ crossings.

To further elucidate the role of mitochondrial dynamics in the expansion of the mutant mtDNA, we used yeast strains with disrupted mitochondrial fusion and fission machinery. We found that hyperfusion of mitochondrial network caused by a deletion of *DNM1* gene, which encodes a key component of mitochondrial fission machinery (Bleazard et al., 1999), increased the percentage of *grande* colonies in *HS rho*$^-$×*rho*$^+$ crossings (Fig. 2C). However, we found that, in contrast to FCCP treatment, this effect was most likely due to the increased frequency of spontaneous loss of HS mtDNA in the *Δdnm1* background (Fig. 2D). At the same time, FCCP did not change the ratio of *grande*-to-*petite* diploid colonies in *Δdnm1 HS rho*$^-$×*Δdnm1 rho*$^+$ crossings. To exclude the effect of spontaneous loss of mtDNA, we mated our strains of the wild-type (*WT*)

Journal of Cell Science (2017) 130, 1274-1284 doi:10.1242/jcs.197269

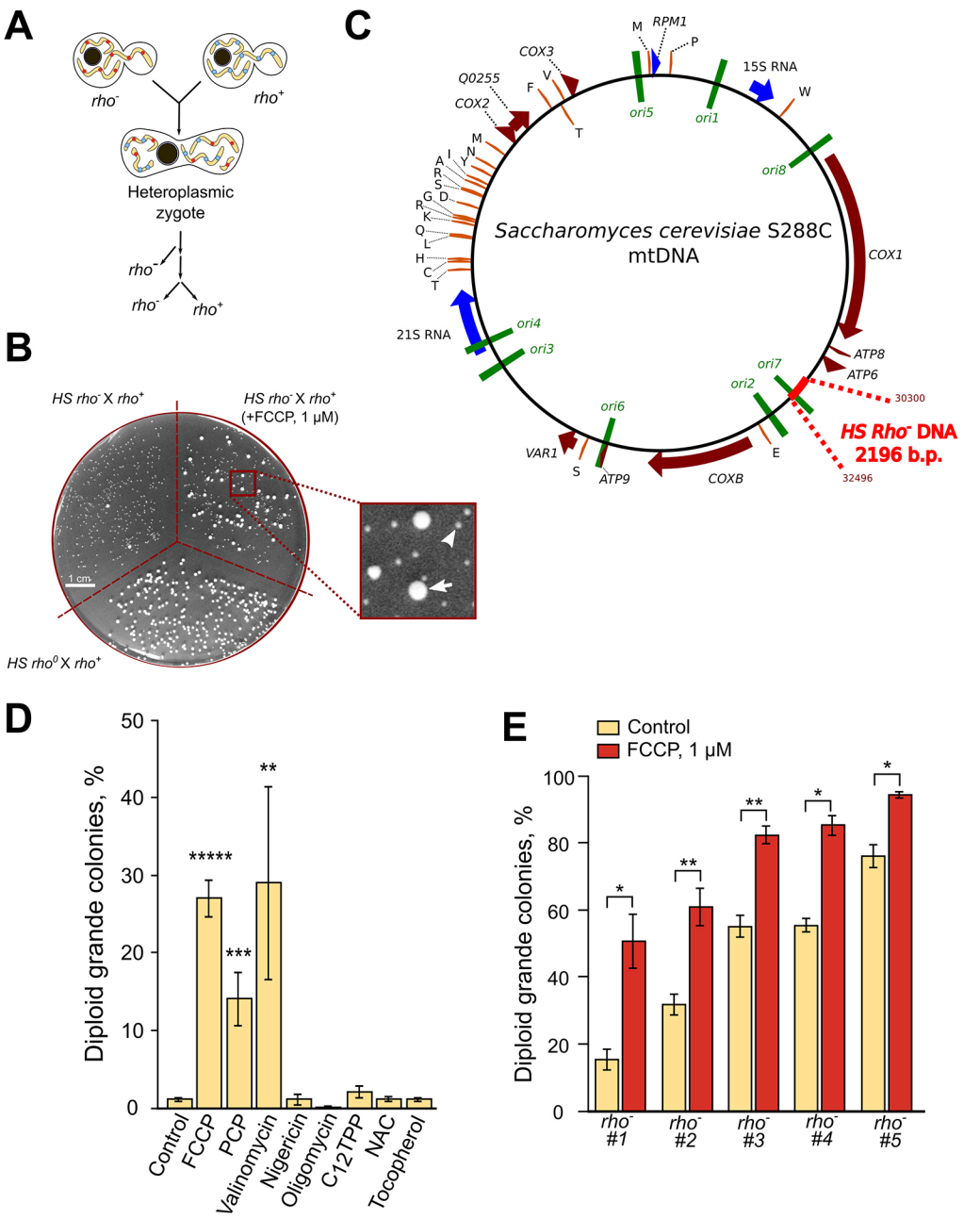

Fig. 1. Dissipation of transmembrane potential increases the numbers of *grande* diploid cells in *rho*⁻×*rho*⁺ mating assays. (A) Scheme illustrating the assay for measuring mtDNA suppressivity. (B) Representative photograph of the grown colonies. The lower third corresponds to the control rho^0×rho^+ crossing, where rho^0 is a derivative strain of *HS rho*⁻ (see Material and Methods). The top two thirds correspond to *HS rho*⁻×*rho*⁺ crossings, with addition of FCCP in the upper-right third. The magnification shows *grande* (arrow) and *petite* (arrowhead) colonies. (C) A map of the complete *Saccharomyces cerevisiae* mitochondrial DNA. The bright red color highlights the region that has been preserved in the *HS rho*⁻ strain. (D) The effects of mitochondrial inhibitors, antioxidants and rapamycin on suppressivity of *HS rho*⁻ strain. Final concentrations: FCCP, 1 μM; pentachlorophenol (PCP), 10 μM; valinomycin, 1 μM; nigericin, 2 μM; oligomycin, 5 μg/ml; dodecyl triphenylphosphonium (C12TPP), 2 μM; N-acetylcysteine (NAC), 5 mM; tocopherol, 50 μM; control, 1% ethanol. Results are mean ±s.e.m. (*n* biological repeats from left to right=28, 26, 8, 4, 3, 3, 3, 6 and 3). $^{**}P<0.01$; $^{***}P<0.001$; $^{*****}P<10^{-7}$ (Mann–Whitney *U*-test with Bonferroni correction). (E) The effect of FCCP is not limited to a specific *rho*⁻ strain. *rho*⁻ *#1*, *rho*⁻ *#2*, *rho*⁻ *#3*, *rho*⁻ *#5*, strains with wild-type background; *rho*⁻ *#4* - *Δpep4 IDH1-GFP* background. Results are mean ±s.e.m. (*n* biological repeats from left to right=8, 3, 10, 3, 11, 5, 4, 4, 9 and 3). $^{*}P<0.05$; $^{**}P<0.01$ (Mann–Whitney *U*-test).

background in the presence of the Dnm1 inhibitor Mdivi-1 (50 μM) (Cassidy-Stone et al., 2008). As, in this case, the inhibition of mitochondrial fission was temporary, such an approach allowed us to prevent the loss of mtDNA by the *rho*⁻ strain (Fig. 2D). We found that in the presence of Mdivi-1, the FCCP-mediated decrease of suppressivity was abolished (Fig. 2C). This observation shows that mitochondrial fission is required for the anti-suppressivity effect of the uncouplers. Moreover, we showed that upregulation of yeast mitofusin gene *FZO1* partially abolished the FCCP-mediated decrease of suppressivity, while the inhibition of mitochondrial fusion by repression of *FZO1* did not significantly affect the suppressivity (Fig. 2C). These results are in line with the idea that hyperfusion of mitochondria in the zygotes promotes clonal expansion of the selfish mtDNA variant in the case of FCCP treatment. Importantly, in the above experiments, we mated a *rho*⁺ strain with a deleted *DNM1* gene and containing the *FZO1* gene under the control of an inducible GAL-promoter (P_{GAL}) with the *HS rho*⁻ strain of *WT* background. The selection of the strains for this experiment was dictated by the following reasons: (1) deletion or repression of the *FZO1* gene induces a very rapid destabilization of mitochondrial DNA in the wild-type background, while allowing preservation of full-length mtDNA in the *Δdnm1* background (Bleazard et al., 1999); (2) according to the accepted model, the presence of Fzo1p on the outer membranes of the both mitochondria is required for their fusion (Anton et al., 2011); (3) in the background of our strain, transformation of P_{GAL} promoter cassette in *Δdnm1 HS rho*⁻ strain induces loss of mtDNA. Thus, to test the effect of *FZO1*, we repressed the gene only in one of the mating strains.

We found that the HS mtDNA clonal expansion in the zygotes produced by mating of the P_{GAL}-*FZO1 Δdnm1 rho*⁺ strain with the *WT HS rho*⁻ strain in glucose-containing medium (P_{GAL} repression conditions) can be inhibited by FCCP as in the case of the control *HS rho*⁻ strain (Fig. 2C). At the same time, YPRafGal medium

Journal of Cell Science (2017) 130, 1274-1284 doi:10.1242/jcs.197269

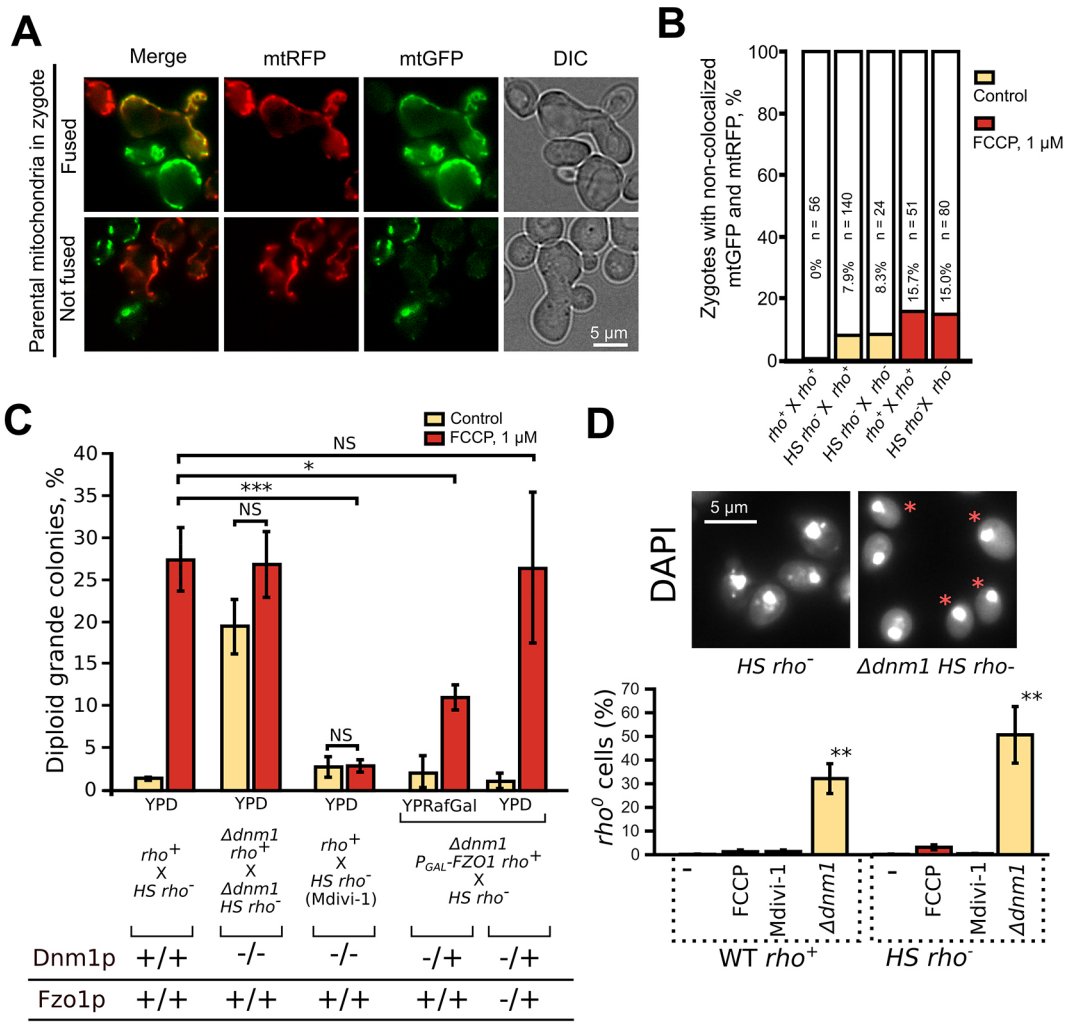

Fig. 2. Disruption of mitochondrial fission inhibits the effect of FCCP on suppressivity. (A) Representative images of *HS rho*$^{-}$ × *wt rho*$^{+}$ zygotes with fused and non-fused mitochondria. Each strain contained either mitochondrially targeted (mt)GFP or mtRFP on a plasmid under control of an inducible GAL-promoter. (B) Quantification of the experiments on different crossings in the presence or absence of uncoupler. FCCP (1 µM) partially blocks the fusion of the parental mitochondria during yeast mating. (C) The deletion of the *DNM1* gene (Δ*dnm1*) or inhibition of Dnm1p by Mdivi-1 (50 µM) abrogates the effect of FCCP (1 µM) on *HS rho*$^{-}$ suppressivity. Simultaneous repression of mitofusin *FZO1* (as occurs for P_{GAL} on YPD medium) and deletion of *DNM1* does not abrogate the effect of FCCP. The lower table represents the expected activity of the corresponding gene product in a zygote due to repression or inhibition (i.e. -/-, indicates fully inhibited, -/+ indicates one wild-type copy and one inhibited or deleted copy, and +/+ indicates two wild-type copies). Results are mean±s.e.m. (*n* biological repeats from left to right=26, 26, 8, 8, 7, 9, 3, 3, 3 and 3). **P*<0.05; *****P*<0.0001; NS, not significant (Mann–Whitney *U*-test with Bonferroni correction). (D) Analysis of the presence of mitochondrial DNA in the control and *HS rho*$^{-}$ strains. The photograph on the top represents HS *rho*$^{-}$ (left) and HS *rho*$^{-}$ *Δdnm1* and *rho*^{0} *Δdnm1* (right) cells stained with DAPI. Red asterisks mark *rho*^{0} cells without visible DAPI signal outside the nuclei. The graph on the bottom represents the percentage of *rho*^{0} cells for indicated conditions [the untreated strain (-), strains treated with 1 µM FCCP or 50 µM or Mdivi-1, and the untreated *Δdnm1* strain]. Results are mean±s.e.m. (*n* biological repeats from left to right=7, 4, 3, 6, 7, 8, 3, 3 and 6). ***P*<0.01 (Mann–Whitney *U*-test).

(P_{GAL} overexpression conditions) provides a modest inhibition of the FCCP effect. Taken together, these results indicate that the effect of the uncouplers requires mitochondrial fission, but does not require fusion. This suggests that uncouplers promote the removal of mitochondrial particles carrying HS mtDNA. As mitophagy seemed to be the most likely candidate for such mechanism, we next addressed its role in mediating the effect of the uncouplers.

Mitochondrial degradation by autophagy is activated in heteroplasmic zygotes and is further stimulated by FCCP addition

To test the role of autophagy in the mutant mtDNA transmission in heteroplasmic cells, we looked for the hallmarks of mitochondrial degradation following *rho*$^{+}$×*HS rho*$^{-}$ mating. We produced a number of *rho*$^{+}$ and *rho*$^{-}$ strains lacking the vacuolar protease Pep4, which is required for autophagosomal degradation in vacuoles (Klionsky et al., 1992; Takeshige et al., 1992), and expressing Idh1–GFP to visualize mitochondria (Kanki and Klionsky, 2008; Okamoto et al., 2009). We found that heteroplasmic zygotes (*rho*$^{+}$×*rho*$^{-}$ and *rho*$^{+}$×*rho*^{0}) harbor detectable levels of GFP foci exhibiting Brownian motion within the vacuoles, whereas very few of these structures were present in homoplasmic zygotes (*rho*$^{+}$×*rho*$^{+}$) and haploid cells from the same samples (Fig. 3A,B). FCCP and PCP significantly increased the percentage of the zygotes with GFP foci (Fig. 3C). Notably, in contrast to in the haploid cells, addition of uncouplers in the zygotes also stimulated degradation of mitoGFP (Fig. 3D). In agreement with this, we found that vacuoles of zygotes harbor multimembraneous structures that, as judged by their ultrastructure in transmission electron microscopy images, are likely to be the remnants of digested mitochondria (Fig. 3E). To

Journal of Cell Science (2017) 130, 1274-1284 doi:10.1242/jcs.197269

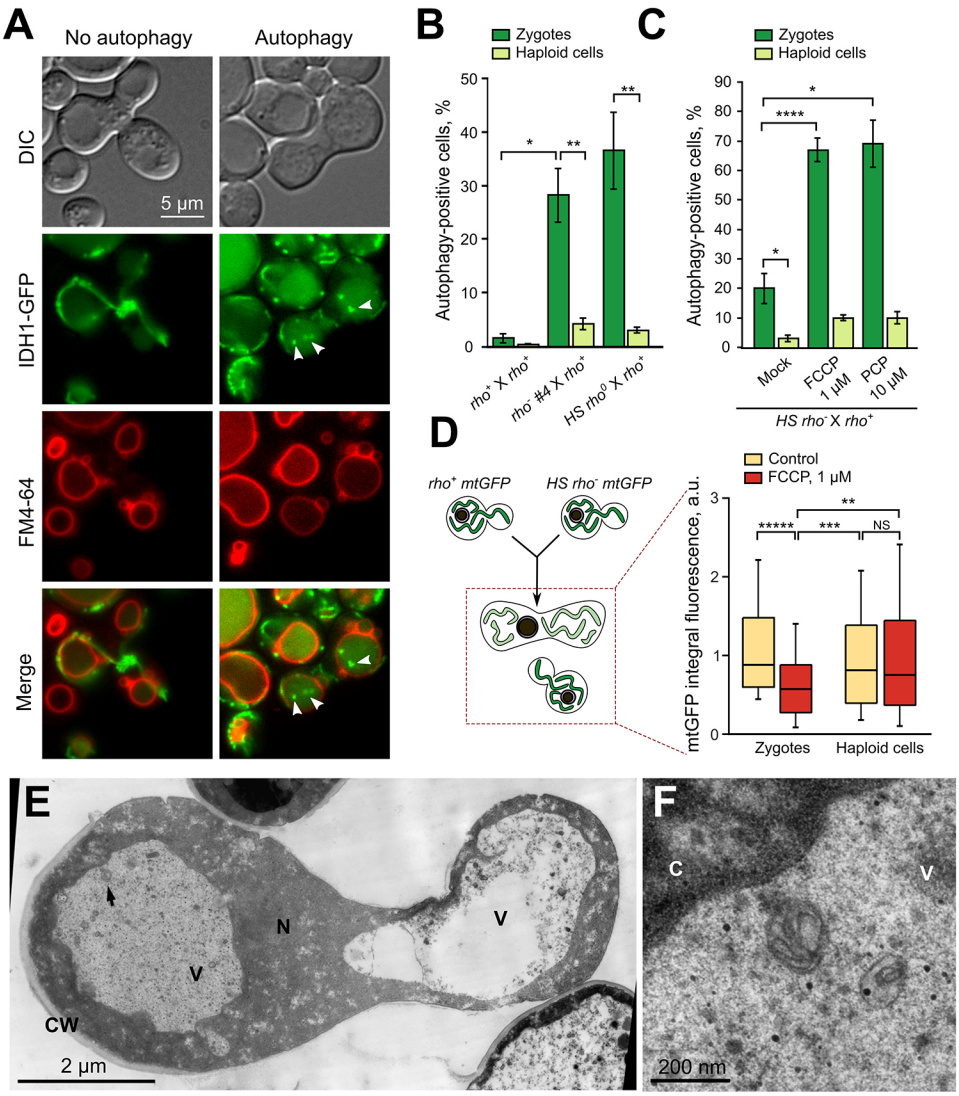

Fig. 3. Mitochondrial degradation is increased in heteroplasmic zygotes and further enhanced by uncoupler treatment. (A) Representative zygotes with and without mitochondrial fragments (white arrowheads) in the vacuolar lumen. Mitochondria are visualized with Idh1–GFP, and vacuolar membranes are stained with FM4-64. (B) Quantification of mitochondrial autophagy activation in heteroplasmic (*rho*$^{-}$ #4×*rho*$^{+}$ and *rho*^{0}×*rho*$^{+}$) and homoplasmic (*rho*$^{+}$×*rho*$^{+}$) zygotes and haploid cells. Although *rho*^{0} strains do not contain any mtDNA, we refer to *rho*^{0}×*rho*$^{+}$ zygotes as heteroplasmic because half of their inherited mitochondria do not contain respiratory chain and remain non-functional after cell mating. Here, all strains had a *Δpep4 IDH1-GFP* background. We counted a cell as mitophagy-positive if at least one GFP foci could be detected in vacuolar lumen. Results are mean±s.e.m. (*n* of biological repeats from left to right=4, 4, 6, 6, 6 and 5). **P*<0.05; ***P*<0.01 (Mann–Whitney *U*-test with Bonferroni correction). (C) Quantification of mitochondrial autophagy activation in heteroplasmic zygotes (*HS rho*$^{-}$×*rho*$^{+}$) and haploid cells treated with FCCP or pentachlorophenol (PCP). Results are mean±s.e.m. (*n* biological repeats from left to right=16, 12, 16, 12, 3 and 3). **P*<0.05; *****P*<0.0001 (Mann–Whitney *U*-test with Bonferroni correction). Here, we used strains with the *Δpep4 IDH1-GFP* background. (D) Assay for mitochondrial GFP (mtGFP) degradation in zygotes. A scheme of the experiment (left) and quantification of the results (right) are shown. Yeast cells overexpressing mtGFP (grown on YPRafGal) were mated in YPD medium in the presence of 1 µM FCCP or with loading control. After 8 h of incubation, integral GFP signals were evaluated for zygotic or non-zygotic single cells (presumably haploid). Total numbers of cells processed in two biological repeats are: zygotes control, 408; zygotes FCCP, 94: haploids control, 1078; haploids FCCP, 572. The box represents the 25–75th percentiles, and the median is indicated. The whiskers show 5–95th percentiles. ***P*<0.01; ****P*<0.001; ******P*<10^{-9}; NS, not significant (Mann–Whitney *U*-test with Bonferroni correction). (E,F) Ultrastructure of yeast zygotes produced by mating of *rho*$^{+}$ *Δpep4 IDH1-GFP*×*HS rho*$^{-}$ *Δpep4 IDH1-GFP* strains in the presence of 1 µM FCCP. Overview of a zygote (E). V, vacuole; C, cytoplasm; CW, fragment of the cell wall; N, nucleus. The arrow points at an intravacuolar multi-membranous inclusion. Enlarged fragment of a zygote (F) displaying fine structural organization of the multi-membranous body.

quantify the data, we scored the number of zygotic cells in 400 90-nm-thick sections. A total of 13 zygotes were detected, eight of which harbored membranous bodies inside the vacuole (Fig. S3) and one of which contained the structure identified as the autophagosome containing the remnants of the mitochondria (Fig. S3E, asterisk). At the same time, none of the 20 cells with non-zygotic morphology examined in the same way displayed membranous bodies within the vacuole (see examples in Fig. S4).

It was important to confirm that mtDNA also enters the vacuoles to be further degraded. We employed confocal microscopy with simultaneous excitation and detection in green and blue channels to visualize both mtDNA and Idh1–GFP. Representative time series, presented by Fig. 4, shows that there is colocalization of Idh1–GFP and DNA signals in a rapidly moving particle within the vacuole. This indicates that mtDNA is also captured by autophagic machinery in the zygotes.

Journal of Cell Science (2017) 130, 1274-1284 doi:10.1242/jcs.197269

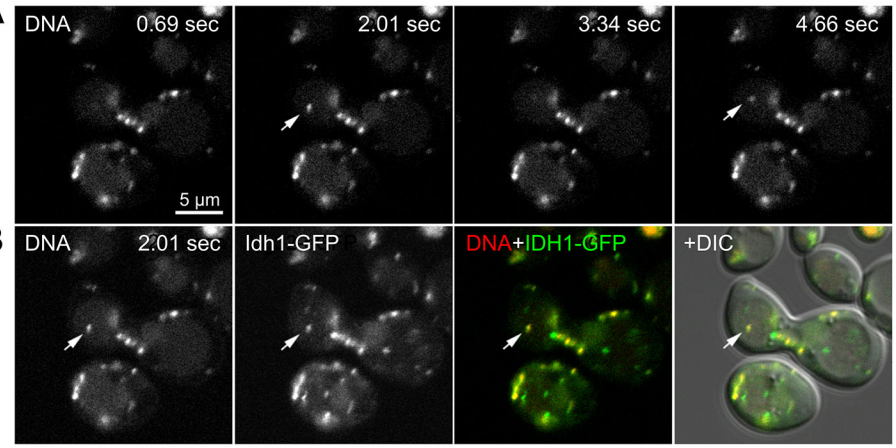

Fig. 4. Simultaneous detection of mitochondrial DNA and the mitochondrial protein IDH1–GFP in the yeast zygote vacuole. (A) Time series showing a DAPI-positive particle diffusion in the vacuole of the zygote (DAPI staining). (B) Multichannel image showing colocalization of DAPI and IDH1–GFP signals. The white arrow marks DAPI-stained foci in vacuolar lumen. *HS rho*$^{-}$ and *rho*$^{+}$ cells (*Δpep4 IDH1-GFP* background) were mixed in the presence of FCCP (1 µM) and DAPI (5 µg/ml) and left for mating as in a standard protocol. After 30 h, the cells were washed with water supplemented with DAPI (5 µg/ml) and analyzed by performing confocal microscopy (see Materials and Methods). Strains used were: *rho*$^{+}$ *Δpep4 IDH1-GFP*×*HS rho*$^{-}$ *Δpep4 IDH1-GFP*.

Is the induction of mitochondrial fission required for the effect of FCCP on mitochondrial degradation? To answer this, we measured the percentage of zygotes with vacuolar GFP foci in the matings of *rho*$^{+}$ and *HS rho*$^{-}$ with the *Δdnm1* background or under Mdivi-1 treatment. Mitochondrial degradation in zygotes was activated in these experiments to the same extent as in the control experiment (Fig. 5A,B).

Next, we studied the role of mitochondrial autophagy machinery in mitochondria degradation in heteroplasmic yeast zygotes treated with the uncoupler FCCP. We produced *rho*$^{+}$ and *HS rho*$^{-}$ derivative strains with the deletion of *ATG8* or with conditional regulation (through P_{GAL}) of the autophagy-related genes *ATG11*, *ATG32* and *ATG33*. Atg8 plays an important role in autophagosome formation and is essential for selective and non-selective types of autophagy (Lang et al., 1998; Okamoto et al., 2009). Atg11 functions as an adapter protein and is needed for different types of selective autophagy (Kanki and Klionsky, 2008). *ATG32* and *ATG33* are required for selective mitophagy, for example during nitrogen starvation or cultivation at the post-log phase, and are not required for other types of selective and non-selective autophagy (Kanki et al., 2009a,b). Deletion of *ATG8* and repression of *ATG32* or both *ATG32* and *ATG33* weakened the effect of FCCP on the suppressivity (Fig. 5C,D). At the same time, repression of ATG genes decreased the number of zygotes with GFP foci in the vacuolar lumen. A decrease was observed both in the absence and presence of FCCP (Fig. 5E). The percentages of zygotes containing vacuolar foci in the mutant strains were significantly lower than in the wild-type strain under either condition (Fig. 5E). However, in *ATG8* and P_{GAL}-*ATG11* mutants, we detected bright foci with higher signal intensities adjacent to vacuoles in zygotes produced by autophagy mutants (Fig. 5A,E).

Our data show that *ATG8* gene deletion prevented the formation of vacuolar GFP foci, while the FCCP-mediated inhibition of *HS rho*$^{-}$ clonal expansion was still significant in the same strains (Fig. 5D,E). It is possible that, although the tested mutants did not execute normal mitochondrial autophagy, mitochondrial fragments can still be partially isolated from the rest of mitochondrial network, thus preventing the inheritance of mtDNA carried by such fragments.

Taken together, our data can be explained by a depolarization-mediated increase of selectivity of mitochondria degradation. Are there any other possible explanations? In fact, it is possible that the activation of non-selective mitochondria degradation can increase the chances of segregation of the wild-type variant of mtDNA during the zygote division. Indeed, several rounds of cell division can be required to complete the replacement of the wild-type mtDNA by the *HS rho*$^{-}$ selfish variant. Moreover, a single copy of selfish mtDNA inherited by a daughter of heteroplasmic zygote could be sufficient for the eventual replacement of the wild-type mtDNA in all progeny of this cell. Therefore, a significant decrease in total mtDNA copy number could increase the chances of the forming bud exclusively harboring the wild-type mtDNAs.

To distinguish between these possibilities, we tested the combined effect of uncoupling and inhibition of the respiratory chain by using the respiratory chain complex III inhibitors antimycin A and myxothiazole. We reasoned that if uncouplers activate mtDNA quality control, then inhibiting the respiratory chain of functional mitochondria with the *rho*$^{+}$ variant of mtDNA would 'blind' this mechanism and abolish the effect of FCCP in heteroplasmic diploid cells. Alternatively, if non-specific mitophagy is responsible for the effect, additional treatment with respiration inhibitors would have either no effect or increase the percentage of *grande* colonies in *HS rho*$^{-}$ × *rho*$^{+}$ crossings. We found that the antimycin A moderately decreased the effect of FCCP, while myxothiazol showed a statistically insignificant effect in the same direction (Fig. 6A).

Next, to test possible selectivity of mitophagy in zygotes towards non-functional mitochondrial DNAs, we compared the numbers of DAPI-positive vacuolar foci in *rho*$^{+}$×*rho*$^{-}$ and *rho*$^{+}$×*rho*^{0} crossings. We found that there was a significantly higher number of zygotes with DAPI-positive dots produced by mating of *rho*$^{+}$*Δpep4 IDH1-GFP* and *rho*$^{-}$ *Δpep4 IDH1-GFP* strains than in the experiments with *rho*^{0} strains (Fig. 6B). The effect was similar in non-treated zygotes as well as in the zygotes produced in the presence of FCCP. This result suggests that mutant mtDNAs are more likely to be captured by mitophagy than wild-type ones.

DISCUSSION

Here, we report that uncouplers induce degradation of mitochondria in zygotes and that this can affect the result of competition between selfish (hypersuppressive) and wild-type variants of mtDNA. This effect is inhibited in yeast strains with repressed mitophagy genes *ATG32* and *ATG33*, as well as in the strains with compromised core autophagy machinery. Moreover, the deletion of mitochondrial fission gene *DNM1* or inhibition of the corresponding protein by the low-molecular-mass inhibitor Mdivi-1 prevented the effect of the uncoupler on the mutant mtDNA clonal expansion. In the mammalian cells, mitochondrial dynamics is tightly linked to the quality control of mitochondria, and depolarized mitochondria are routed towards autophagic degradation (Twig and Shirihai, 2011;

Journal of Cell Science (2017) 130, 1274-1284 doi:10.1242/jcs.197269

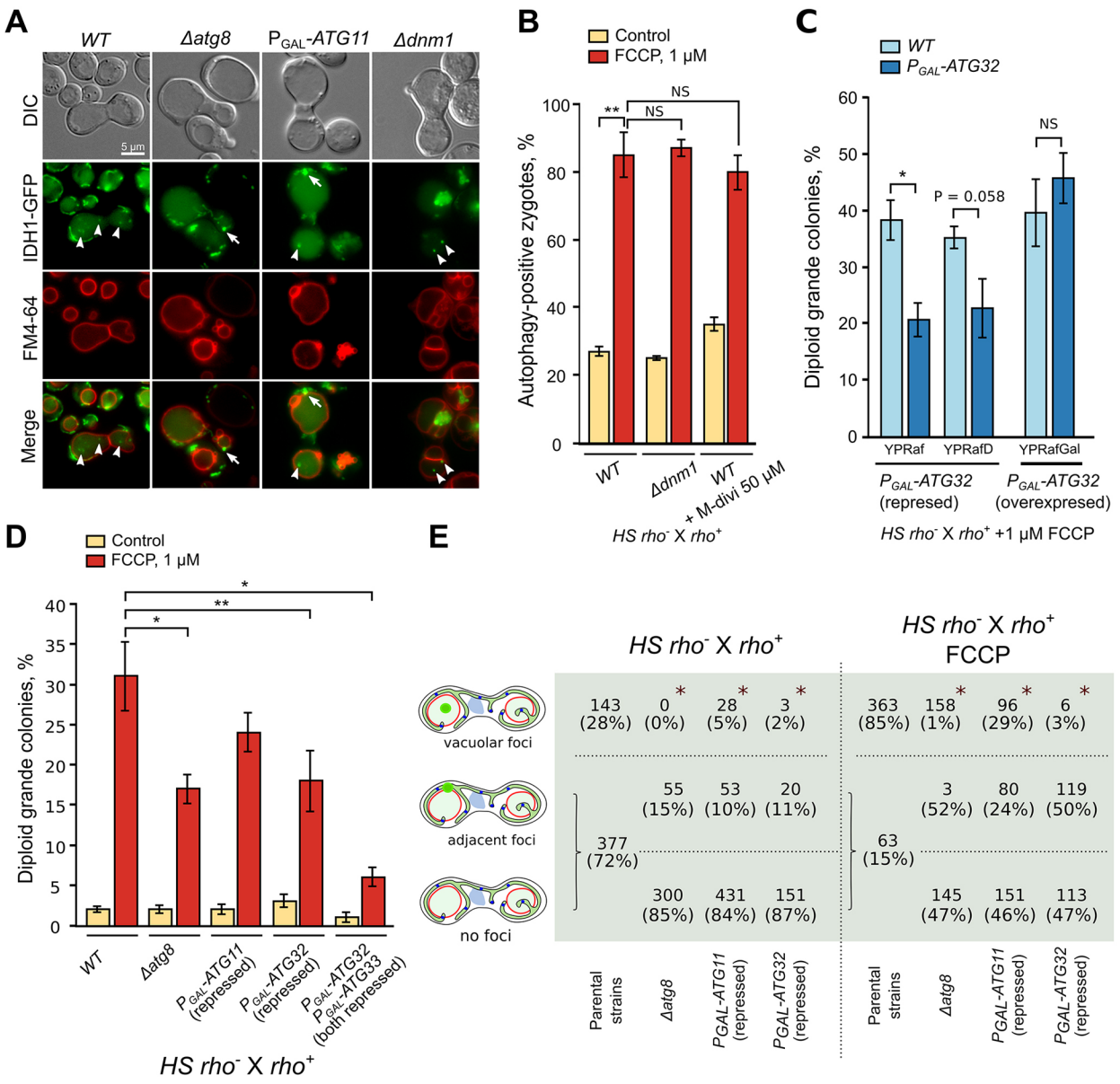

Fig. 5. Repression of the autophagy-related genes *ATG8, ATG11, ATG32* or *ATG33* decreases both mitochondrial autophagy and the effect of uncouplers on suppressivity. (A) Representative zygotes with different types of mitochondrial autophagy. Zygotes with GFP foci in vacuolar lumen (white arrowhead, *WT, Δdnm1, P_{GAL}-ATG11*) and adjacent to the vacuole (white arrow, *Δatg8, P_{GAL}-ATG11*). P_{GAL}-*ATG11* is indicative of repression of ATG11 by growth on YPD medium. Mitochondria are visualized with IDH1–GFP; vacuolar membranes are stained with FM4-64. (B) Quantification of mitochondrial autophagy activation in the zygotes with disrupted mitochondrial fission (*Δdnm1* or Mdivi-1 treatment) as detected by the presence of GFP foci in the vacuoles. Here, we used strains with a *Δpep4 IDH1-GFP* background. Results are mean±s.e.m. (*n* biological repeats from left to right=7, 7, 3, 3, 6 and 6). ***P*<0.01 (Mann–Whitney *U*-test). (C) The decrease of the effect of uncouplers in the P_{GAL}-*ATG32* strain is not due to the growth on YPRafGal medium but due to the repression of *ATG32* gene. The effect of FCCP on suppressivity was partially decreased in ATG32-repressing medium for P_{GAL}-*ATG32* strains but not for *WT* strains in cases of crossings of *HS rho*$^{-}$×*rho*$^{+}$, indicating that the decrease is due to the lack of *ATG32*. YPRafD (2% raffinose, 0.5% glucose), YPRaf (2% raffinose), YPRafGal (2% raffinose 1% galactose). **P*<0.05; NS, not significant (Mann–Whitney *U*-test). Here, we used P_{GAL}-*ATG32* strains in a wild-type background. The standard errors of the mean of five biological repeats are shown. (D) The effect of FCCP on suppressivity is partially decreased in the strains lacking *ATG8*, *ATG11*, *ATG32* or *ATG33*. For this experiment, we used *ATG8*, *ATG11* and *ATG32* mutants in a *Δpep4 IDH1-GFP* background and *ATG32-ATG33* double mutants in a wild-type background. Results are mean±s.e.m. (*n* biological repeats from left to right=10, 9, 12, 10, 11, 10, 23, 23, 4 and 4). **P*<0.05; ***P*<0.01 (Mann–Whitney *U*-test with Bonferroni correction). (E) Quantification of the different types of GFP foci in zygotes with repressed ATG genes under control conditions or upon treatment with FCCP (1 µM). The zygotes without vacuolar foci and with distinguishable adjacent GFP foci were counted as a separate category, but considered as 'no foci' for statistical analysis. In these experiments, we used strains with a *Δpep4 IDH1-GFP* background. **P*<10^{-13} according to χ-squared test for independency of vacuolar foci compared to the parental strain. The numbers of zygotes of different types were pooled from experiments conducted on four separate days.

Twig et al., 2008; Wei et al., 2015). In yeast, mitophagy induced by the deletion of phosphosphingolipid phospholipase gene *ISC1* requires the dynamin-related protein Dnm1p, the key component of the mitochondrial fission machinery (Teixeira et al., 2015). However, the well studied starvation-induced mechanisms of autophagic mitochondria degradation do not require mitochondrial fission and are not sensitive to uncoupling (Mendl et al., 2011). Interestingly, in our work, mitochondrial fission was found to be dispensable for the activation of mitophagy in the presence of uncouplers. This observation is in line with earlier work

Journal of Cell Science

Journal of Cell Science (2017) 130, 1274-1284 doi:10.1242/jcs.197269

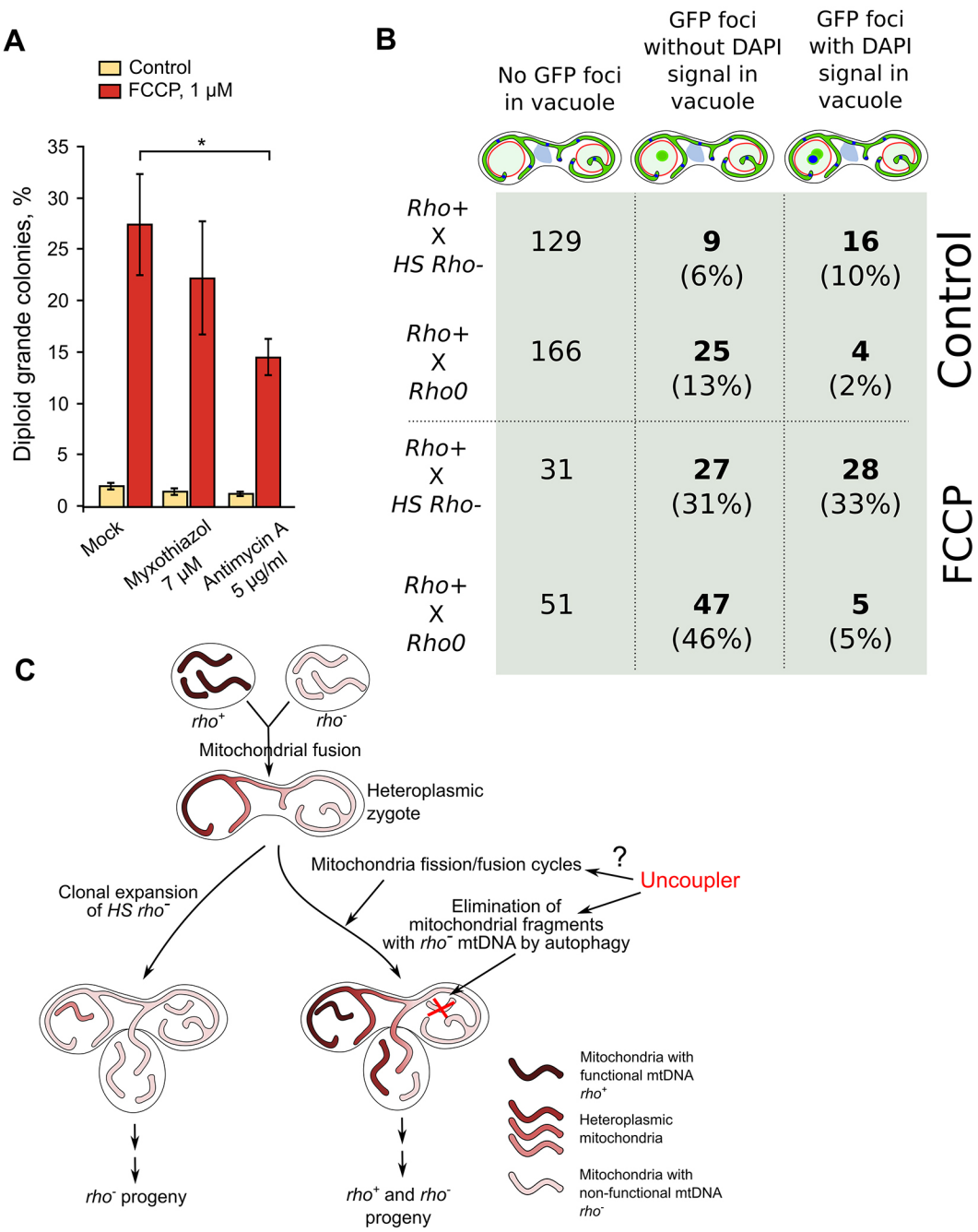

Fig. 6. Hypothetical scheme for the mechanisms underlying the effect of uncouplers on *rho*⁻ mtDNA suppressivity. (A) Treatment with the respiratory chain inhibitor antimycin A combined with FCCP partially decreases the effect of the uncoupler on *HS rho*⁻ suppressivity in *HS rho*⁻×*rho*⁺ crossings. Results are mean±s.e.m. (*n* biological repeats from left to right=10, 10, 9, 9, 10 and 10). **P*<0.05 (Mann–Whitney *U*-test with Bonferroni correction). (B) Yeast zygotes produced by fusion of *HS rho*⁻ and *rho*⁺ cells display a higher frequency of DAPI signal in the vacuoles than the zygotes produced by mating of *rho*⁺ and *rho*⁰ cells. The table represents the numbers of zygotes of each type found in experiments conducted on five separate days. In these experiments, all haploid cells expressed Idh1–GFP as a mitochondrial marker and carried a knockout of *PEP4* to prevent instant GFP degradation in the vacuole. The crossings were performed in the presence of DAPI (see Materials and Methods). A zygote was considered GFP positive if at least one GFP foci was found in it, whereas the zygote was considered DAPI positive if at least one of GFP foci was DAPI positive (see Materials and Methods). We did not detect any DAPI-positive but GFP-negative zygotes. *P*-values for χ-squared tests for the independence for *rho*⁰×*rho*⁺ crossings compared to *rho*⁻×*rho*⁺ crossings are below 5×10^{-4} for both control and FCCP conditions. (C) Scheme representing the effect of uncouplers on *rho*⁻ mtDNA clonal expansion in heteroplasmic zygotes.

by Mendl and co-authors, who showed that the previously reported role of mitochondrial division gene *FIS1* can actually be attributed to a secondary mutation in TOR-pathway regulator *WHI2* (Mendl et al., 2011). While both processes are required for protection from selfish mtDNAs, they appear to be activated independently. We did not see any inhibition of autophagy in *Δdnm1* strains or upon inactivation of Dnm1p by Mdivi-1 (Fig. 5B). Taken together, our observations imply the existence of a quality control mechanism in yeast zygotes that requires mitochondrial fission and autophagy (see Fig. 6C). The obtained data can be also explained by facilitated mitochondria turnover that increases the chances of segregation of yeast cells harboring only the wild-type mtDNA. The low amount of zygotes

Journal of Cell Science (2017) 130, 1274-1284 doi:10.1242/jcs.197269

with DAPI signal in vacuolar lumen produced by $rho^{+}\times rho^{0}$ cells (Fig. 6B) is consistent with the selective mechanism. Fig. 2 shows that the soluble mitochondrial GFP is relatively quickly equilibrated in the yeast zygotes, which might not be the case for integral inner membrane proteins encoded by mitochondrial DNA. It is possible that even a small difference of transmembrane potential can drive effective selection of normal over mutant mtDNA. However, as the two proposed explanations are not mutually exclusive, we suggest that both can take place in zygotes. Nevertheless, to our knowledge, the obtained results for the first time show that nuclear-encoded mitochondria degradation machinery opposes the clonal expansion of selfish mutant mtDNA in a microorganism.

Inhibitors of the respiratory chain have been shown to induce bulk autophagy in yeast cells, but required the selective autophagy receptor Atg32 (Deffieu et al., 2013). In that work, Deffieu and co-authors found that prolonged incubation of yeast cells in the presence of the uncoupler CCCP also induced GFP–Atg8 proteolysis (Deffieu et al., 2013), although the effect was much less pronounced than in the case of treatment with myxothiazole. Uncouplers dissipate energy in mitochondria and, therefore, theoretically, can induce an unspecific starvation response, which is known to induce macroautophagy (Tal et al., 2007). However, the inhibition of ATP synthase by oligomycin did not provide any detectable advantage for the wild-type variant of mtDNA (Fig. 1C). Moreover, it was shown previously that induction of autophagy in yeast caused by mitochondrial dysfunction is not mediated by a decrease in cytoplasmic ATP levels (Priault et al., 2005). Therefore, in our experimental system, the induction of autophagy is most likely mediated by one of the mitochondria-to-nucleus signaling pathways initiated by a decrease of transmembrane potential, which in turn regulates the export of mitochondrial metabolites from the matrix to the cytoplasm (for a review, see Eisenberg-Bord and Schuldiner, 2016). Indeed, treatment of yeast cells with uncouplers induces changes in gene expression (Epstein et al., 2001), and some of the changes can activate mitophagy.

We did not observe any strong effects of uncouplers on non-mated haploid cells in our experimental system (Fig. 3C,D); the effect was specific to zygotes. While the molecular mechanism of such specificity is not clear, there are obvious benefits for yeast cells to keep the proposed mechanism of the quality control functional in zygotes rather than in haploids. For a haploid cell, selfish mitochondrial DNA can be produced due to *de novo* mutation or acquired via cytoduction during mating. mtDNA mutation frequency in yeasts is high only in laboratory strains, whereas, in the wild, the number of yeast strains with *petite* mutations is relatively low (Dimitrov et al., 2009). Thus, the risk of selfish mtDNA invasion is especially high during mating. Therefore, it seems possible that fungi developed a mechanism that upregulates mitochondrial quality control specifically in zygotes and/or their first diploid descendants. Interestingly, in species with a biparental type of mtDNA inheritance, selfish mitochondrial plasmids can invade the experimental and the wild-type populations (Clark et al., 2012; Phillips et al., 2015).

To summarize, we found that mitochondrial depolarization inhibits clonal expansion of selfish mtDNAs. This effect requires functional mitochondrial autophagy mechanisms and mitochondrial fission. Our observations are in a good agreement with the data on facilitated degradation of mitochondria in germline cells of species with uniparental inheritance of mitochondrial DNA (for a review, see Sato and Sato, 2013). Moreover, our data could provide a background for application of uncouplers as a treatment against diseases associated with mitochondrial DNA heteroplasmy.

MATERIALS AND METHODS

Yeast strains and plasmids

Yeast strains used in this study are listed in Tables S2 and S3. All strains are derivatives of *W303-1A* (*ade2-101 his3-11 trp1-1 ura3-52 can1-100 leu2-3*, *112*, *GAL*, *psi+*, *MATa*) or *W303-1B* (*ade2-101 his3-11 trp1-1 ura3-52 can1-100 leu2-3*, *112*, *GAL*, *psi+*, *MATα*). To delete complete open reading frames by homologous recombination, the *HIS3MX6* cassette was amplified from pFA6a-HIS3MX6 plasmid (Wach et al., 1997) and the KanMX6 cassette from pFA6a-KanMX6 (Wach et al., 1994) with the gene-specific primers. The GAL-promoter and N-terminal GFP tag were inserted into the specific genomic loci by homologous recombination of PCR-amplified modules from plasmids pFA6a-GFP(S65T)-TRP1, pFA6a-HIS3MX6-PGAL1 or pFA6a-KanMX6-PGAL1 (Longtine et al., 1998) with the gene-specific primers. All strains were checked by genome-based PCR with gene-specific primers. For expressing mitochondrially targeted GFP and RFP, pYX223-mtGFP (Westermann and Neupert, 2000) and pYX223-mtRFP plasmids were used. pYX223-mtRFP plasmid was previously obtained in our laboratory by ligation of RFP-encoding sequence excised from pTagRFP-N (Evrogen, Moscow, Russia) with HindIII and BamHI into HindIII and BamHI restriction sites of the pYX223-mtGFP plasmid. Transformation of yeast strains was performed by the lithium acetate method.

rho^{-} yeast strains were generated by selection of spontaneous *petite* clones. Importantly, S288C-based yeast strains display high frequencies of mtDNA deletions due to a deleterious polymorphism in the mitochondrial DNA polymerase genes (Dimitrov et al., 2009). To select rho^{-} clones, we plated aliquots of exponentially growing yeast cells on solid YPDGly (0.1% D-glucose and 2% glycerol) medium. On this medium, rho^{-} *petite* cells form distinguishably smaller colonies than rho^{+} *grande* cells. The absence of growth on a non-fermantable carbon source (YPGly) was tested for each selected strain. To visualize mtDNA and distinguish between rho^{-} and rho^{0} genotypes, we stained yeast cells with DAPI (see Fig. 2D for examples). First, we fixed cells with 70% ethanol and incubated for 30 min with DAPI (0.1 µg/ml). Strains containing clearly distinguishable DAPI-positive dots in cytoplasm were considered rho^{-}. rho^{0} strains were produced by incubation of a parental strain overnight in YPD containing 25 µg/ml ethidium bromide (EB) at 30°C. Then the cultures were plated on solid YPDGly medium and individual *petite* clones were selected. The absence of mitochondrial DNA was confirmed by fluorescence microscopy using DAPI (see see Fig. 2D for an example).

Growth conditions and reagents

Yeast cells were grown in rich growth media (YPD, yeast peptone D-glucose; YPRaf, yeast peptone raffinose; YPGal, yeast peptone galactose; YPGly, yeast peptone glycerol; YPDGly, yeast peptone D-glucose glycerol) prepared according to Sherman (2002) or in synthetic medium prepared according to the manufacturer's (Sigma-Aldrich) protocol. Yeast extract was obtained from BD; bactoagar, bactopeptone and D-glucose were from Amresco; DAPI was from Molecular Probes (Life Technologies); raffinose was from Alfa Aesar. Other chemicals were obtained from Sigma-Aldrich.

Yeast fusion assay for determination of suppressivity

To generate heteroplasmic yeast zygotes, cells of opposite mating types (i.e. *MATa* and *MATα*) containing different genome-encoded selectable markers (*LEU2* and *URA3*, respectively), one of which carries normal mtDNA (rho^{+}) and the other mutant mtDNA (rho^{-}) were grown in rich medium to log-phase. Then strains of opposing mating types were mixed in equal proportions to give a final optical density at 550 nm (OD_{550})=0.1 (2×10^{6} cells/ml) for the mixture. Compounds of interest or ethanol were added to the mixture if needed. Then, the mixtures were left at room temperature for yeast mating. After 20 h, the mixtures were diluted 100–1000 times with sterile distilled water and plated on solid YNB-LEU-URA double-selective medium with 0.1% glucose and 2% glycerol as the carbon source. The number of colonies was counted after 2–3 days. The suppressivity of the rho^{-} strain used in the mating assay was calculated as the percentage of *petite* colonies grown after the mating.

Fluorescence microscopy

Yeast cells were visualized by using an Olympus BX51 microscope (U-MNIBA3 filter for GFP, U-MNU2 filter for DAPI and U-MNG2 filter for FM4-64). Photographs were taken with a DP30BW CCD camera.

Mitophagy assay

To monitor mitophagy activation in heteroplasmic zygotes or haploid cells during mating, we performed our mating assay using yeast strains expressing chromosomally encoded IDH1–GFP. The protein is a GFP-tagged version of a subunit of isocitrate dehydrogenase that is localized in the mitochondrial matrix; we used it to visualize mitochondria. To prevent rapid degradation of mitochondrial fragments in vacuoles, we also deleted the gene *PEP4*, encoding one of the main vacuolar hydrolases, in these strains. The cells were analyzed by using fluorescence microscopy after 20 h following mixing of the strains. The percentages of zygotes and haploid cells containing fluorescent GFP foci in the vacuolar lumen were calculated.

Assay for monitoring *in vivo* mitochondrial fusion

Yeast strains containing either pYX233-mtGFP or pYX233-mtRFP plasmids were grown overnight to the log-phase in liquid YNB-HIS RafGal medium for the expression of mitochondrially targeted fluorescent proteins. Then, the suspensions of the strains of opposite mating types expressing different fluorescent proteins were mixed to obtain an equal proportion of each strain in the suspension and a cell concentration of 2×10^6 cells/ml. Sterile 20% glucose solution was added to the mixture to give a final concentration of glucose equal to 2% to repress the expression of the fluorescent proteins. FCCP (or an equal volume of ethanol) was added to the mixture to a final concentration of 1 µM and the mixture was then left at room temperature for 6 h for zygote formation. Then the percentage of zygotes (that had already formed the first bud to ensure that mating had occurred) with non-fused mitochondrial networks was calculated by using fluorescence microscopy. Fusion of mitochondrial networks of the parental cells in zygotes was scored as positive in cases of full colocalization of GFP and RFP signals.

mtGFP degradation assay

Yeast strains containing the pYX233-mtGFP plasmid were treated as for the *in vivo* mitochondrial fusion assay with the exception that cells were left at room temperature for 8 h for zygote formation. After 8 h, fluorescent images of the cells were taken with the same exposure time for the control and FCCP-treated suspensions. The images were analyzed with ImageJ software. Integral fluorescence intensities of zygotes and haploid cells were calculated and divided by the mean integral fluorescence intensities of all measured cells (zygotes plus haploid cells) for each experiment in each condition. The experiments were performed in two biological repeats.

FM4-64 staining

To visualize yeast vacuolar membranes, cells were stained with 0.8 µM FM4-64 (Molecular Probes) at 30°C for 20 min in YPD, then washed twice with sterile distilled water, resuspended in fresh YPD medium and incubated at 30°C for 90–120 min.

Confocal microscopy

Confocal microscopy was performed with a Nikon C2 confocal microscope (Nikon Corporation, Japan) with a Nikon Plan Apo VC 60×1.40 NA oil immersion lens. Simultaneous excitation was performed using 403 and 487 nm lasers for DAPI and eGFP respectively, with detection in blue and green channels. A green laser (561 nm) was used to obtain a non-descanned DIC image with the transmission detector. Image size was 256×256 pixels at 90 nm per pixel with pinhole size of 60 µm (2.9 AUs for blue channel). For each cell, ten frames were recorded at 0.75 s per frame with an 800 ms interval between acquisitions.

Electron microscopy

For electron microscopy studies, suspensions of yeast cells were washed in PBS to remove culture medium and fixed with cold 2.5% solution of glutaraldehyde (SPI) in 100 mM sodium cacodylate (SPI) for 40 min. Fixed samples were thoroughly washed with sodium cacodylate solution and subjected to 45 units per ml lyticase (Sigma-Aldrich) treatment in 1.4 M sorbitol solution supplemented with 20 mM triethanolamine, 1 mM calcium chloride and 10 mM DTT for 45 min at 30°C under gentle agitation.

Cell wall lysis solution was removed by centrifugation (600 ***g*** for 5 min) and cells were washed several times in sodium cacodilate before post fixation with 1% osmium tetroxide in sodium cacodylate for 20 min. Cells were then dehydrated in increasing concentrations of ethanol, including a 40 min impregnation with uranyl-acetate in 70% ethanol for 40 min. Then they were transferred to anhydrous acetone and infiltrated with Epon-812 resin (SPI) by treatment with increasing concentrations of resin in acetone. Samples were then transferred into pure resin and incubated for 48 h at 70°C.

The fixed cells were then mounted on formvar-coated copper slot-grids. Ultrathin 80 nm sections were prepared with a glass knife using a Reichert-Jung Ultracut E ultra-microtome (Reichert-Jung, Austria). Sections were post-stained with 2% aqueous solution of uranyl-acetate and with lead citrate.

Samples were examined and photographed with a JEM-1400 electron microscope (Jeol, Japan) running at 100 kV. Images were captured using a bottom-mounted Quemesa digital camera (Olympus Soft Imaging Solutions, Germany).

Statistical data analysis

All data were summarized as means±s.e.m. and statistical significance was assessed using Mann–Whitney *U*-test with Bonferroni adjustments for multiple comparisons. *n* in the figure legends indicates the number of replicated experiments performed on separate days unless otherwise specified.

Acknowledgements

The authors are grateful to anonymous reviewers for their comments and in particular for the suggestion to perform an experiment depicted on Fig. 6B.

Competing interests

The authors declare no competing or financial interests.

Author contributions

Conceptualization: I.E.K., D.A.K.; Methodology: I.E.K., S.A.G., S.S.S., D.A.K.; Validation and Formal analysis: I.E.K., D.A.K.; Investigation: I.E.K., S.A.G., S.S.S., E.A.S., D.A.K.; Writing – original draft preparation: D.A.K., I.E.K.; Writing – review and editing: D.A.K., F.F.S., I.E.K., S.A.G.; Visualization: I.E.K., S.A.G., D.A.K.; Supervision: D.A.K., F.F.S.; Funding acquisition: D.A.K., F.F.S.

Funding

The suppressive *rho*$^-$ strains (Fig. 1) were produced and characterized with the support of Russian Science Foundation (grant 14-50-00029). The mitochondrial dynamics experiments (Fig. 2) were supported by Russian Foundation for Basic Research (grant 16-04-01381); the rest of the work (Figs 3–6) was supported by Russian Science Foundation (grant 14-24-00107). This research was partly carried out using the equipment provided by Lomonosov Moscow State University development program PNR5.13.

Supplementary information

Supplementary information available online at
http://jcs.biologists.org/lookup/doi/10.1242/jcs.197269.supplemental

References

Aanen, D. K. and Maas, M. F. P. M. (2012). Recruitment of healthy mitochondria fuels transmissible cancers. *Trends Genet.* **28**, 1-6.

Allen, J. F. (2015). Why chloroplasts and mitochondria retain their own genomes and genetic systems: colocation for redox regulation of gene expression. *Proc. Natl. Acad. Sci. USA* **112**, 10231-10238.

Anton, F., Fres, J. M., Schauss, A., Pinson, B., Praefcke, G. J. K., Langer, T. and Escobar-Henriques, M. (2011). Ugo1 and Mdm30 act sequentially during Fzo1-mediated mitochondrial outer membrane fusion. *J. Cell Sci.* **124**, 1126-1135.

Bleazard, W., McCaffery, J. M., King, E. J., Bale, S., Mozdy, A., Tieu, Q., Nunnari, J. and Shaw, J. M. (1999). The dynamin-related GTPase Dnm1 regulates mitochondrial fission in yeast. *Nat. Cell Biol.* **1**, 298-304.

Cassidy-Stone, A., Chipuk, J. E., Ingerman, E., Song, C., Yoo, C., Kuwana, T., Kurth, M. J., Shaw, J. T., Hinshaw, J. E., Green, D. R. et al. (2008). Chemical inhibition of the mitochondrial division dynamin reveals its role in Bax/Bak-

dependent mitochondrial outer membrane permeabilization. *Dev. Cell* **14**, 193-204.

Clark, K. A., Howe, D. K., Gafner, K., Kusuma, D., Ping, S., Estes, S. and Denver, D. R. (2012). Selfish little circles: transmission bias and evolution of large deletion-bearing mitochondrial DNA in Caenorhabditis briggsae nematodes. *PLoS ONE* **7**, e41433.

Contamine, V. and Picard, M. (2000). Maintenance and integrity of the mitochondrial genome: a plethora of nuclear genes in the budding yeast. *Microbiol. Mol. Biol. Rev.* **64**, 281-315.

de Zamaroczy, M., Marotta, R., Faugeron-Fonty, G., Goursot, R., Mangin, M., Baldacci, G. and Bernardi, G. (1981). The origins of replication of the yeast mitochondrial genome and the phenomenon of suppressivity. *Nature* **292**, 75-78.

Deffieu, M., Bhatia-Kiššová, I., Salin, B., Klionsky, D. J., Pinson, B., Manon, S. and Camougrand, N. (2013). Increased levels of reduced cytochrome b and mitophagy components are required to trigger nonspecific autophagy following induced mitochondrial dysfunction. *J. Cell Sci.* **126**, 415-426.

Dimitrov, L. N., Brem, R. B., Kruglyak, L. and Gottschling, D. E. (2009). Polymorphisms in multiple genes contribute to the spontaneous mitochondrial genome instability of Saccharomyces cerevisiae S288C strains. *Genetics* **183**, 365-383.

Eisenberg-Bord, M. and Schuldiner, M. (2016). Ground control to major TOM: mitochondria-nucleus communication. *FEBS J.* **284**, 196-210.

Ephrussi, B., de Margerie-Hottinguer, H. and Roman, H. (1955). Suppressiveness: a new factor in the genetic determinism of the synthesis of respiratory enzymes in yeast. *Proc. Natl. Acad. Sci. USA* **41**, 1065-1071.

Epstein, C. B., Waddle, J. A., Hale, W., Davé, V., Thornton, J., Macatee, T. L., Garner, H. R. and Butow, R. A. (2001). Genome-wide responses to mitochondrial dysfunction. *Mol. Biol. Cell* **12**, 297-308.

Fangman, W. L., Henly, J. W., Churchill, G. and Brewer, B. J. (1989). Stable maintenance of a 35-base-pair yeast mitochondrial genome. *Mol. Cell. Biol.* **9**, 1917-1921.

Greaves, L. C., Nooteboom, M., Elson, J. L., Tuppen, H. A. L., Taylor, G. A., Commane, D. M., Arasaradnam, R. P., Khrapko, K., Taylor, R. W., Kirkwood, T. B. L. et al. (2014). Clonal expansion of early to mid-life mitochondrial DNA point mutations drives mitochondrial dysfunction during human ageing. *PLoS Genet.* **10**, e1004620.

He, Y., Wu, J., Dressman, D. C., Iacobuzio-Donahue, C., Markowitz, S. D., Velculescu, V. E., Diaz, L. A., Jr, Kinzler, K. W., Vogelstein, B. and Papadopoulos, N. (2010). Heteroplasmic mitochondrial DNA mutations in normal and tumour cells. *Nature* **464**, 610-614.

Higuchi-Sanabria, R., Charalel, J. K., Viana, M. P., Garcia, E. J., Sing, C. N., Koenigsberg, A., Swayne, T. C., Vevea, J. D., Boldogh, I. R., Rafelski, S. M. et al. (2016). Mitochondrial anchorage and fusion contribute to mitochondrial inheritance and quality control in the budding yeast Saccharomyces cerevisiae. *Mol. Biol. Cell* **27**, 776-787.

Kanki, T. and Klionsky, D. J. (2008). Mitophagy in yeast occurs through a selective mechanism. *J. Biol. Chem.* **283**, 32386-32393.

Kanki, T., Wang, K., Cao, Y., Baba, M. and Klionsky, D. J. (2009a). Atg32 is a mitochondrial protein that confers selectivity during mitophagy. *Dev. Cell* **17**, 98-109.

Kanki, T., Wang, K., Baba, M., Bartholomew, C. R., Lynch-Day, M. A., Du, Z., Geng, J., Mao, K., Yang, Z., Yen, W.-L. et al. (2009b). A genomic screen for yeast mutants defective in selective mitochondria autophagy. *Mol. Biol. Cell* **20**, 4730-4738.

Klionsky, D. J., Cueva, R. and Yaver, D. S. (1992). Aminopeptidase I of Saccharomyces cerevisiae is localized to the vacuole independent of the secretory pathway. *J. Cell Biol.* **119**, 287-299.

Kmiec, B., Woloszynska, M. and Janska, H. (2006). Heteroplasmy as a common state of mitochondrial genetic information in plants and animals. *Curr. Genet.* **50**, 149-159.

Lang, T., Schaeffeler, E., Bernreuther, D., Bredschneider, M., Wolf, D. H. and Thumm, M. (1998). Aut2p and Aut7p, two novel microtubule-associated proteins are essential for delivery of autophagic vesicles to the vacuole. *EMBO J.* **17**, 3597-3607.

Ling, F. and Shibata, T. (2004). Mhr1p-dependent concatemeric mitochondrial DNA formation for generating yeast mitochondrial homoplasmic cells. *Mol. Biol. Cell* **15**, 310-322.

Longtine, M. S., McKenzie, A., III, Demarini, D. J., Shah, N. G., Wach, A., Brachat, A., Philippsen, P. and Pringle, J. R. (1998). Additional modules for versatile and economical PCR-based gene deletion and modification in Saccharomyces cerevisiae. *Yeast* **14**, 953-961.

Lorimer, H. E., Brewer, B. J. and Fangman, W. L. (1995). A test of the transcription model for biased inheritance of yeast mitochondrial DNA. *Mol. Cell. Biol.* **15**, 4803-4809.

Meeusen, S., McCaffery, J. M. and Nunnari, J. (2004). Mitochondrial fusion intermediates revealed in vitro. *Science* **305**, 1747-1752.

Mendl, N., Occhipinti, A., Muller, M., Wild, P., Dikic, I. and Reichert, A. S. (2011). Mitophagy in yeast is independent of mitochondrial fission and requires the stress response gene WHI2. *J. Cell Sci.* **124**, 1339-1350.

Michaelis, G., Douglass, S., Tsai, M.-J. and Criddle, R. S. (1971). Mitochondrial DNA and suppressiveness of petite mutants in Saccharomyces cerevisiae. *Biochem. Genet.* **5**, 487-495.

Müller, M., Lu, K. and Reichert, A. S. (2015). Mitophagy and mitochondrial dynamics in Saccharomyces cerevisiae. *Biochim. Biophys. Acta* **1853**, 2766-2774.

Okamoto, K., Kondo-Okamoto, N. and Ohsumi, Y. (2009). Mitochondria-anchored receptor Atg32 mediates degradation of mitochondria via selective autophagy. *Dev. Cell* **17**, 87-97.

Pernice, W. M., Vevea, J. D. and Pon, L. A. (2016). A role for Mfb1p in region-specific anchorage of high-functioning mitochondria and lifespan in Saccharomyces cerevisiae. *Nat. Commun.* **7**, 10595.

Phillips, W. S., Coleman-Hulbert, A. L., Weiss, E. S., Howe, D. K., Ping, S., Wernick, R. I., Estes, S. and Denver, D. R. (2015). Selfish mitochondrial DNA proliferates and diversifies in small, but not large, experimental populations of Caenorhabditis briggsae. *Genome Biol. Evol.* **7**, 2023-2037.

Priault, M., Salin, B., Schaeffer, J., Vallette, F. M., di Rago, J.-P. and Martinou, J.-C. (2005). Impairing the bioenergetic status and the biogenesis of mitochondria triggers mitophagy in yeast. *Cell Death Differ.* **12**, 1613-1621.

Sato, M. and Sato, K. (2013). Maternal inheritance of mitochondrial DNA by diverse mechanisms to eliminate paternal mitochondrial DNA. *Biochim. Biophys. Acta* **1833**, 1979-1984.

Severin, F. F., Severina, I. I., Antonenko, Y. N., Rokitskaya, T. I., Cherepanov, D. A., Mokhova, E. N., Vyssokikh, M. Y., Pustovidko, A. V., Markova, O. V., Yaguzhinsky, L. S. et al. (2010). Penetrating cation/fatty acid anion pair as a mitochondria-targeted protonophore. *Proc. Natl. Acad. Sci. USA* **107**, 663-668.

Sherman, F. (2002). Getting started with yeast. *Methods Enzymol.* **350**, 3-41.

Solignac, M., Monnerot, M. and Mounolou, J. C. (1983). Mitochondrial DNA heteroplasmy in Drosophila mauritiana. *Proc. Natl. Acad. Sci. USA* **80**, 6942-6946.

Stewart, J. B. and Chinnery, P. F. (2015). The dynamics of mitochondrial DNA heteroplasmy: implications for human health and disease. *Nat. Rev. Genet.* **16**, 530-542.

Takeshige, K., Baba, M., Tsuboi, S., Noda, T. and Ohsumi, Y. (1992). Autophagy in yeast demonstrated with proteinase-deficient mutants and conditions for its induction. *J. Cell Biol.* **119**, 301-311.

Tal, R., Winter, G., Ecker, N., Klionsky, D. J. and Abeliovich, H. (2007). Aup1p, a yeast mitochondrial protein phosphatase homolog, is required for efficient stationary phase mitophagy and cell survival. *J. Biol. Chem.* **282**, 5617-5624.

Taylor, R. W. and Turnbull, D. M. (2005). Mitochondrial DNA mutations in human disease. *Nat. Rev. Genet.* **6**, 389-402.

Taylor, S. D., Ericson, N. G., Burton, J. N., Prolla, T. A., Silber, J. R., Shendure, J. and Bielas, J. H. (2014). Targeted enrichment and high-resolution digital profiling of mitochondrial DNA deletions in human brain. *Aging Cell* **13**, 29-38.

Teixeira, V., Medeiros, T. C., Vilaça, R., Pereira, A. T., Chaves, S. R., Côrte-Real, M., Moradas-Ferreira, P. and Costa, V. (2015). Ceramide signalling impinges on Sit4p and Hog1p to promote mitochondrial fission and mitophagy in Isc1p-deficient cells. *Cell. Signal.* **27**, 1840-1849.

Twig, G. and Shirihai, O. S. (2011). The interplay between mitochondrial dynamics and mitophagy. *Antioxid. Redox Signal.* **14**, 1939-1951.

Twig, G., Elorza, A., Molina, A. J. A., Mohamed, H., Wikstrom, J. D., Walzer, G., Stiles, L., Haigh, S. E., Katz, S., Las, G. et al. (2008). Fission and selective fusion govern mitochondrial segregation and elimination by autophagy. *EMBO J.* **27**, 433-446.

Wach, A., Brachat, A., Pöhlmann, R. and Philippsen, P. (1994). New heterologous modules for classical or PCR-based gene disruptions in Saccharomyces cerevisiae. *Yeast* **10**, 1793-1808.

Wach, A., Brachat, A., Alberti-Segui, C., Rebischung, C. and Philippsen, P. (1997). Heterologous HIS3 marker and GFP reporter modules for PCR-targeting in Saccharomyces cerevisiae. *Yeast* **13**, 1065-1075.

Wei, H., Liu, L. and Chen, Q. (2015). Selective removal of mitochondria via mitophagy: distinct pathways for different mitochondrial stresses. *Biochim. Biophys. Acta* **1853**, 2784-2790.

Westermann, B. and Neupert, W. (2000). Mitochondria-targeted green fluorescent proteins: convenient tools for the study of organelle biogenesis in Saccharomyces cerevisiae. *Yeast* **16**, 1421-1427.

Wonnapinij, P., Chinnery, P. F. and Samuels, D. C. (2008). The distribution of mitochondrial DNA heteroplasmy due to random genetic drift. *Am. J. Hum. Genet.* **83**, 582-593.

Ye, K., Lu, J., Ma, F., Keinan, A. and Gu, Z. (2014). Extensive pathogenicity of mitochondrial heteroplasmy in healthy human individuals. *Proc. Natl. Acad. Sci. USA* **111**, 10654-10659.

Journal of Cell Science